S©MR

СИБИРСКИЕ ЭЛЕКТРОННЫЕ
МАТЕМАТИЧЕСКИЕ ИЗВЕСТИЯ
Siberian Electronic Mathematical Reports
http://semr.math.nsc.ru
ISSN 1813-3304

Vol. ??, No. ?, pp. ??? (2025)
https://doi.org/10.33048/semi.2023.20.???

УДК 532.135
MSC 76A10

ON THE STABILITY OF THE PLANE FLOW OF VISCOELASTIC POLYMER LIQUID

R.E. SEMENKO AND **G.N. SHUKUROV**

Communicated by ?.?. ??

Abstract: We have studied the spectral problem for plane Poiseuille-type flow of viscoelastic polymer liquid. The flow was modelled with the equations of rheological Vinogradov–Pokrovskii model. The numerical spectral procedure was used to calculate eigenvalues of the problem and to determine the critical values of parameters where the instability of the flow occurs. It was shown that the critical Reynolds number goes to well-known value of approximately 5772 (that is the critical value for the viscous fluid) while the relaxation time goes to zero. The slight increase of elastic properties of the fluid (or Weissenberg number) leads to rapid increase of critical Reynolds number, while further increase of Weissenberg number destabilizes the flow by pushing the critical Reynolds number to zero. Similar to a number of other rheological models, the Vinogradov–Porkovskii model demonstrates the elastic instability effect, that is the spectral problem has unstable modes that are not a continuation of unstable modes of the viscous newtonean flow.

Keywords: Vinogradov–Pokrovskii rheological model, Poiseuille flow, spectral problem.

Semenko R.E., Shukurov G.N., On the stability of the plane flow of viscoelastic polymer liquid.

The study of Semenko R.E. was carried out within the framework of the state contract of the Sobolev Institute of Mathematics (project no. FWNF-2022-0008).

Received, Published.

1 Introduction

Polymer solutions and melts are viscoelastic fluids, and the viscoelasticity causes the number of features not typical for viscous newtonean fluids. Among these features are shear-thinning effects, growth of extensional viscosity, stress relaxation in non-stationary flows and many others [1, 2]. One field of the particular interest within the theory of viscoelastic fluids is the stability properties of the flows of certain geometries. The recent experimental studies of polymer solutions [3, 4] showed that the addition of small amounts of polymer in the solution causes complex influence on the stability of the flows which include both transition delay to turbulence (the transition happens with higher Reynolds numbers compared to pure viscous flows), but also the early turbulence effect which on the contrary reduces the critical Reynolds number.

Among the rheological models of polymer dynamics probably the most well-researched one is the famous Oldroyd-B model [5]. Over the years the extensive research was performed for it and its simplified forms like upper-convected Maxwell model (UCM) [6, 7, 8, 9]. But Oldroyd-B model by itself is not without flaws due to relatively simple linear constitutive equations, which leads to shear-rate independent viscosity, unbounded growth of extensional viscosity and several other properties which does not fit well with known experimental data [10]. There are large number of more advanced models which addresses these flaws but the knowledge of their properties is much more limited.

One way to improve the adequacy of the modeling of viscoelastic flows is mesoscopic approach which takes into account both general experimental observations and dynamics of separate long macromolecules of polymer [11, 12]. The relatively recent modified Vinogradov–Pokrovskii model (mVP) already demonstrated good agreement with experiment in several viscometric flows [13, 14, 15, 16], but the understanding of the stability properties for this model is quite limited so far, partially due to mathematical complexity of the governing equations of the model. Saying that, some existing results indicate that even basic flows within this model could be notoriously unstable. There are evidences that the stationary flows in the plane channels and tubes and even the state of the rests could be linearly unstable, which put a question regarding the adequacy of the model [17, 18, 19]. On the other hand, numerical simulations performed in [20] for plane Poiseuille-type flow in mVP model showed good stabilization of non-stationary solutions on equilibrium states over time at least for relatively low Reynolds and Weissenberg numbers. Granted, that simulations were taken for simplified problem formulation with fixed pressure gradient and transverse velocity, but nonetheless this evidence promote more thorough study of linear stability of the problem.

One way to check the adequacy of stability research is to study how the equations behave for low Weissenberg numbers. Since the zero relaxation time (and thus zero Weissenberg number) should transform the spectral

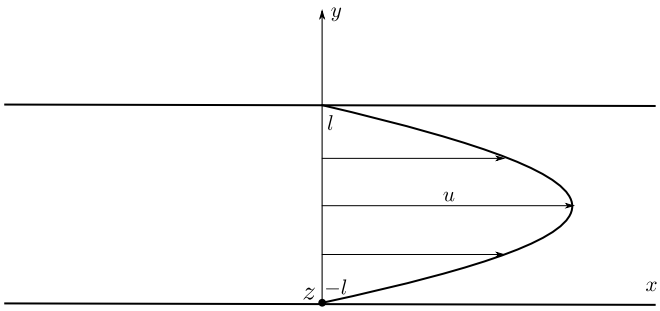

FIG. 1. Flow in the plane channel.

problem to the one for pure viscous flow, the results should also correlate with known information regarding the stability of Poiseuille flow for Navier–Stokes equations, including the critical Reynolds number of approximately $\mathrm{Re} \approx 5772$. In the present research we show the numerical results of the stability problem, including the limit case of low Weissenberg number. We discuss the nature of discovered instabilities and compare the results with the ones for viscous Poiseuille flow.

2 Problem statement

Let us introduce the problem for linear stability of the steady plane flow between two parallel plates. Assuming vector $\boldsymbol{u} = (u, v, w)^\top$ to be the velocity of the flow in $(x, y, z)^\top$ space and $-l < y < l$ to be the flat channel, consider the flow shown on Fig. 1, driven by the pressure gradient along the x-axis. The plates $y = \pm l$ are fixed and no-slip conditions for the flow are imposed at them. The continuity equation and momentum equations for incompressible fluid are naturally

$$\mathrm{div}\boldsymbol{u} = u_x + v_y + w_z = 0, \tag{1}$$

$$\rho \frac{\mathrm{d}\boldsymbol{u}}{\mathrm{d}t} = \mathrm{div}\sigma, \tag{2}$$

here ρ is the constant density and σ is the viscoelastic stress tensor. Also

$$\frac{\mathrm{d}}{\mathrm{d}t} = \frac{\partial}{\partial t} + (\boldsymbol{u}, \nabla).$$

The stress tensor is split into the isotropic and anisotropic parts

$$\sigma = -pI + \Pi,$$

where p is the pressure, I is the unity tensor and $\Pi = \{a_{jk}\}$, $j, k = 1, 2$ is the symmetrical tensor of anisotropy (tensor of additional stresses) [11]. The tensor Π represents the effects of viscous and elastic forces of the flow. We will use non-dimensional form of the governing equations with the scales l for length, u_H for velocity and l/u_H for time, where u_H is the velocity of the steady flow at the central line of the channel. The pressure is scaled with

ρu_H^2, and the anisotropic stresses are scaled with $\eta_0 u_H/l$, where η_0 is the initial viscosity [11].

The mVP model utilizes the mesoscopic approach, that is it deliver the rheological constitutive equation from the stochastic motion of one polymer chain within the anisotropic viscous media. The assumption is that the source of that anisotropy is the stretch of the chain along the flow, and thus the anisotropy is connected to the orientation of the chain. In simplest single mode case which we are using here the chain is reduced to single "dumbbell" and the orientation of the chain is determined by one vector. The components of Π are the moments of the coordinates of this vector [1, 2]. The anisotropic drag coefficient of the media Θ is determined as a nonlinear function of spherical and deviatoric parts of Π with phenomenological parameters k and β respectively [11, 12]:

$$\Theta \sim \left(I + k\left(\frac{\mathrm{Tr}(\Pi)}{3} I\right) + \beta\left(\Pi - \frac{\mathrm{Tr}(\Pi)}{3} I\right)\right)^{-1}.$$

Naturally, the coefficient k represent the amount of anisotropy due to the size of the polymer dumbbell, and β reflects the impact of its orientation. According to [21], the sensible ratio between them is $k = 1.2\beta$ which fits well with experimental measurements.

The constitutive equation of single mode mVP is

$$\frac{\mathrm{d}\Pi}{\mathrm{d}t} - (\nabla \boldsymbol{u})^{\top}\Pi - \Pi(\nabla \boldsymbol{u}) + k\mathrm{Re}\left(\frac{\mathrm{Tr}(\Pi)}{3}\right)\Pi + \\ + \beta\mathrm{Re}\left(\Pi - \frac{\mathrm{Tr}(\Pi)}{3} I\right)\Pi + \frac{\Pi}{\mathrm{W}} = \frac{\nabla \boldsymbol{u} + (\nabla \boldsymbol{u})^{\top}}{\mathrm{ReW}}. \quad (3)$$

Here $\mathrm{Re} = \rho u_H l/\eta_0$ is the Reynolds number, $\mathrm{W} = \tau_0 u_H/l$ is the Weissenberg number, τ_0 is the relaxation time. It can be seen that the coefficients k and β are attached to the nonlinear terms of (3). This particular type of nonlinearity is what defines mVP among other rheological models. For instance, (3) transforms to constitutive equation of UCM model if $k = \beta = 0$.

The equations (1)-(3) are supplemented with boundary conditions

$$\boldsymbol{u}(y = \pm 1) = 0. \quad (4)$$

First let us introduce the steady-state solution in plane channel for this model. Assume that

$$u = u_0(y),\ v = w = 0,\ a_{jk} = a_{jk0}(y),\ j,k = 1,2,\ a_{j3} = 0,\ j = 1,2,3, \quad (5)$$

then from (2) we have

$$p = p_0(x,y,z) = p(y) - Ax,$$

where $p(y)$ is an unknown function, A is the constant pressure gradient.

Following [20, 22], we have

$$a_{120}(y) = -Ay,$$

$$\left(\frac{2k+\beta}{3}\right))a_{220}^3+\left(1+\frac{2k+\beta}{3}\right)a_{220}^2/(\mathrm{ReW})+$$
$$+\left((1/(\mathrm{ReW})^2+\frac{2k+\beta}{3}a_{120}^2\right)a_{220}+(\beta/(\mathrm{ReW}))a_{120}^2=0. \quad (6)$$

The (6) provides the values of $a_{220}(y)$ as the roots of cubic equation with variable coefficients. It was shown in [20] that only one root of this equation could lead to potentially stable solution, and that root satisfies the condition $a_{220}(0)=0$. Sticking with this solution, the $a_{110}(y)$ is found from

$$a_{110}=a_{220}+\frac{2a_{120}^2}{1/(\mathrm{ReW})+a_{220}}.$$

Finally, $u_0(y)$ is calculated from

$$u_0'=\frac{\hat{K}_I a_{120}}{a_{220}+1/(\mathrm{ReW})} \quad (7)$$

with boundary condition $u_0(-1)=0$. The condition $u(1)=0$ would be satisfied automatically due to the symmetry of $u(y)$ [20]. Here and further on the derivatives by y are marked as strokes,

$$u_0'=\frac{\mathrm{d}u_0}{\mathrm{d}y}.$$

It has to be noted that (5) in general could not be found analytically, unlike the case of simpler models like Oldroyd-B [7, 23, 24]. That means the value of u_H is not known a-priori for a given set of parameters and has to be calculated numerically. Technically that means we have to determine the value of pressure gradient A such that $u_0(0)=1$.

Having the steady solution, now we can formulate the spectral problem for linear stability. Let

$$U_0=(u_0(y),0,0,p_0(x,y),a_{110}(y),a_{120}(y),a_{220}(y),0,0,0)^\top.$$

We are looking for solution of (1)-(4) of the form

$$\hat{U}(t,x,y)=\begin{pmatrix}\hat{u}\\ \hat{v}\\ \hat{w}\\ \hat{p}\\ \hat{a}_{11}\\ \hat{a}_{12}\\ \hat{a}_{22}\\ \hat{a}_{13}\\ \hat{a}_{23}\\ \hat{a}_{33}\end{pmatrix}=U_0+U(y)e^{\lambda t+i\omega x+i\zeta z}, \quad (8)$$

$U(y)=(u(y),v(y),w(y),p(y),a_{11}(y),a_{12}(y),a_{22}(y),a_{13}(y),a_{23}(y),a_{33}(y))^\top$.
Here $\lambda=\lambda_r+i\lambda_i$. The presence of the solutions with $\lambda_r>0$ would indicate the temporal instability of the flow.

Abandoning nonlinear terms, we can obtain the following system for v, w and a_{jk}, $k = 1, 2, 3$.

$$\lambda(v'' - (\omega^2+\zeta^2)v) = -i\omega u_0 v'' + (i\omega(\omega^2+\zeta^2)u_0 + i\omega u_0'')v + \\ + \omega^2 a_{11}' - i\omega a_{12}'' - i\omega(\omega^2+\zeta^2)a_{12} - (\omega^2+\zeta^2)a_{22}' + \\ + 2\omega\zeta a_{13}' - i\zeta a_{23}'' - i\zeta(\omega^2+\zeta^2)a_{23} + \zeta^2 a_{33}', \quad (9)$$

$$\lambda((\omega^2+\zeta^2)w - i\zeta v') = -\omega\zeta u_0 v' + \omega\zeta u_0' v - i\omega(\omega^2+\zeta^2)u_0 w - i\omega^2\zeta a_{11} - \\ - \omega\zeta a_{12}' + i\omega(\omega^2-\zeta^2)a_{13} + \omega^2 a_{23}' + i\omega^2\zeta a_{33}, \quad (10)$$

$$\lambda\omega \mathrm{W} a_{11} = 2i\mathrm{W}a_{120}v'' - 2\omega\left(\frac{1}{\mathrm{Re}} + \mathrm{W}a_{110}\right)v' - \mathrm{W}\omega a_{110}'v - \\ - 2\zeta\mathrm{W}a_{120}w' - 2i\omega\zeta\left(\frac{1}{\mathrm{Re}} + \mathrm{W}a_{110}\right)w - \mathrm{ReW}\omega\frac{k-\beta}{3}a_{110}a_{33} - \\ - \omega\left(2\mathrm{ReW}\frac{k+2\beta}{3}a_{110} + \mathrm{ReW}\frac{k-\beta}{3}a_{220} + iu_0\mathrm{W}\omega + 1\right)a_{11} - \\ - \left(2\beta\mathrm{ReW}\omega a_{120} - 2\mathrm{W}\omega u_0'\right)a_{12} - \mathrm{ReW}\omega\frac{k-\beta}{3}a_{110}a_{22}, \quad (11)$$

$$\lambda\omega \mathrm{W} a_{12} = i\left(\frac{1}{\mathrm{Re}} + \mathrm{W}a_{220}\right)v'' - \left(\mathrm{W}\omega a_{120}' - \left(\frac{1}{\mathrm{Re}} + \mathrm{W}a_{110}\right)i\omega^2\right)v - \\ - \zeta\left(\frac{1}{\mathrm{Re}} + \mathrm{W}a_{220}\right)w' - i\mathrm{W}\omega\zeta a_{120}w - \\ - \mathrm{ReW}\omega\frac{k+2\beta}{3}a_{120}a_{11} - \omega\left(\mathrm{ReW}\frac{k+2\beta}{3}(a_{110}+a_{220}) + i\omega\mathrm{W}u_0 + 1\right)a_{12} - \\ - \mathrm{W}\omega\left(\mathrm{Re}\frac{k+2\beta}{3}a_{120} - u_0'\right)a_{22} - \mathrm{ReW}\omega\frac{k-\beta}{3}a_{120}a_{33}. \quad (12)$$

$$\lambda\mathrm{W}a_{22} = -\mathrm{W}\left(a_{220}' - 2i\omega a_{120}\right)v + 2\left(\frac{1}{\mathrm{Re}} + \mathrm{W}a_{220}\right)v' - \\ - \mathrm{ReW}\frac{k-\beta}{3}a_{220}a_{11} - 2\beta\mathrm{ReW}a_{120}a_{12} - \mathrm{ReW}\frac{k-\beta}{3}a_{220}a_{33} - \\ - \left(i\omega\mathrm{W}u_0 + \mathrm{ReW}\frac{k-\beta}{3}a_{110} + 2\frac{k+2\beta}{3}\mathrm{ReW}a_{220} + 1\right)a_{22} = 0. \quad (13)$$

$$\lambda\mathrm{W}\omega^2 a_{13} = -\frac{\omega\zeta}{\mathrm{Re}}v' + \mathrm{W}\omega^2 a_{120}w' + \omega\left(\frac{i(\omega^2-\zeta^2)}{\mathrm{Re}} + i\mathrm{W}\omega^2 a_{110}\right)w - \\ - \omega^2\left(i\mathrm{W}\omega u_0 + \mathrm{ReW}\frac{k+2\beta}{3}a_{110} + \mathrm{ReW}\frac{k-\beta}{3}a_{220} + 1\right)a_{13} + \\ + \mathrm{W}\omega^2(u_0' - \beta\mathrm{Re}a_{120})a_{23}, \quad (14)$$

$$\lambda \mathrm{W} a_{23} = \frac{i\zeta}{\mathrm{Re}} v + \left(\frac{1}{\mathrm{Re}} + \mathrm{W} a_{220} \right) w' + i\mathrm{W}\omega a_{120} w - \beta \mathrm{ReW} a_{120} a_{13} - \\ - \left(i\mathrm{W}\omega u_0 + \mathrm{ReW} \frac{k-\beta}{3} a_{110} + \mathrm{ReW} \frac{k+2\beta}{3} a_{220} + 1 \right) a_{23}, \quad (15)$$

$$\lambda \mathrm{W} a_{33} = \frac{2i\zeta}{\mathrm{Re}} w - \left(\mathrm{ReW} \frac{k-\beta}{3} (a_{110} + a_{220}) - i\mathrm{W}\omega u_0 + 1 \right) a_{33}. \quad (16)$$

Since the continuity equation should be satisfied at the boundaries of the channel, the system (9)-(16) is supplemented with boundary conditions

$$v(\pm 1) = w(\pm 1) = 0, \; v'(\pm 1) = 0. \quad (17)$$

Remark 1. We should point out that the validity of no-slip conditions (17) for polymer solutions could be disputed since the slipping phenomenon for them is observed under the certain conditions [25, 26]. But we believe the conditions (17) are acceptable for the analysis of the stability properties of the model, even more so that the same conditions are usually assumed for similar research of other rheological models, such as UCM [23, 27], Oldroyd-B [24, 28], FENE-P [29], Giesecus [30] and others, and identical conditions here are essential if the one is going to compare the results of these studies with the present one.

Remark 2. Note that we never specified the pressure gradient A while presented the steady solution U_0. Since we chose the velocity scale u_H to be a maximum value of the velocity, i.e. $u_0(0)$, the constant A should be taken such as $u_0(0) = 1$. For Navier–Stokes equations, and even for some viscoelastic models, this condition simply lead to $A = 2/\mathrm{Re}$. But here the solution U_0 is not known precisely, which does not allow us to get the exact formula for A. Thus we determine A by simple bisection numerical method while numerically integrating the equation (7) from $y = -1$ to $y = 0$.

The problem (9)-(17) has three major parameters: Re, W and β (remember, that the ratio $k = 1.2\beta$ is postulated here according to [21]). It is important to notice that the number W represent the ratio of elastic and viscous forces. If the relaxation time of the media $\tau_0 = 0$ then $\mathrm{W} = 0$ also and the elastic forces are absent. The problem thus would be reduced to the well-known stability problem for the Navier–Stokes equations. Indeed, if $\mathrm{W} = 0$ then from (11)-(13) and (1) we have

$$a_{11} = -\frac{2}{\mathrm{Re}} v' - 2\frac{i\zeta}{\mathrm{Re}} w, \; a_{12} = \frac{i}{\omega \mathrm{Re}} v'' + \frac{i\omega}{\mathrm{Re}} v - \frac{\zeta}{\omega \mathrm{Re}} w, \\ a_{22} = \frac{2}{\mathrm{Re}} v', \; a_{13} = -\frac{\zeta}{\omega \mathrm{Re}} v' + \frac{i}{\omega \mathrm{Re}} (\omega^2 - \zeta^2) w, \\ a_{23} = \frac{i\zeta}{\mathrm{Re}} v + \frac{1}{\mathrm{Re}} w', \; a_{33} = \frac{2i\zeta}{\mathrm{Re}} w.$$

From (9) we then have

$$\lambda(v'' - (\omega^2+\zeta^2)v) + i\omega u_0 v'' - i\omega\left(u_0'' + (\omega^2+\zeta)^2)u_0\right) =$$
$$= \frac{1}{\mathrm{Re}}\left(v^{(4)} - 2(\omega^2+\zeta^2)v'' + (\omega^2+\zeta^2))^2 v\right), \tag{18}$$
$$v(\pm 1) = 0,\ v'(\pm 1) = 0.$$

which would be the known boundary-value problem for Orr-Sommerfeld equation [31] if we would take $\zeta = 0$. The steady solution U_0 for the case $\mathrm{W} = 0$ would also be classical Poiseuille parabolic flow. That fact would allow us to compare the calculations for mVP model for small W with the known results for Navier-Stokes equations.

3 Numerical results

3.1. Calculation of the spectrum. The eigenvalue problem (9)-(17) is solved with the help of spectral method by decomposition of the solution into polynomials on Chebyshev grid. The Chebyshev points on the interval $-1 \le y \le 1$ are

$$y_j = \cos(\pi j/N),\ j = 0, \dots, N.$$

The unknown functions are discretized on that grid, thus transforming into column vectors $\vec{v}$, $\vec{w}$ and $\vec{a}_{jk}$ respectively, and their derivatives are approximated with Chebyshev differential matrix D [32, 33]:

$$v^{(n)} \approx D^n \vec{v}.$$

Let then $\vec{U}$ be a discretized vector of the length $8(N+1)$,

$$\vec{U} = (\vec{v}, \vec{w}, \vec{a}_{11}, \vec{a}_{12}, \vec{a}_{22}, \vec{a}_{13}, \vec{a}_{23}, \vec{a}_{33})^\top.$$

The system of differential equations (9)-(13) then would be transformed into the generalized algebraic eigenvalue problem

$$M_1 \vec{U} = \lambda M_2 \vec{U}, \tag{19}$$

where M_1 and M_2 are some matrices which depend on ω and U_0. The eigenvalues and eigenvectors of (19) are our approximation of the solution of (9)-(17). The problem (19) is solved by the procedure "eig" of MATLAB.

Remark 3. Here we have omitted the details of the way the boundary conditions are approximated. Please refer to the Appendix for that, along with the discussion of the adequacy of the method and possible ways of it's verification.

3.2. Analysis of the unstable modes. We will start the presentation of the results with demonstration of spectra for $\mathrm{Re} = 5000$, which is slightly below the critical value for viscous newtonean fluid, and for various values of W. It would allow us to demonstrate both stabilizing and destabilizing effects of elastic forces on the plane flow. For the purpose of this demonstration we will use $\beta = 0.77$, $\omega = 1$ and $\zeta = 0$.

First let us test the numerical algorithm for $\mathrm{W} = 0$ to compare the results with the one for Navier-Stokes equations. Even if mathematically problems

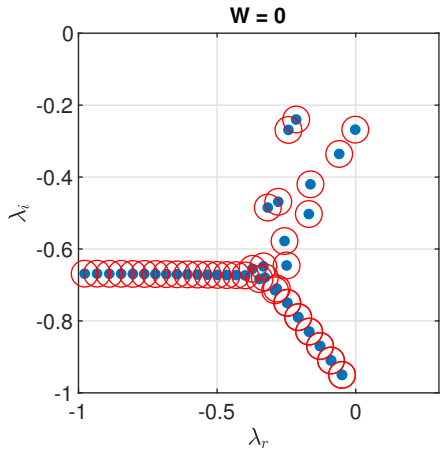

FIG. 2. Spectra of Orr-Sommerfeld equation (red circles) and mVP model at W = 0 (blue dots). Re = 5000, $\beta = 0.77$, $\omega = 1$, $\zeta = 0$.

(9)-(17) and (18) are identical for W = 0, numerically they are not, since the former is the system of second-order equations, while the latter is one equation of forth order. The Fig. 2 shows the calculated spectrum of these two problems, and it can be seen that the spectrum is identical, which is the evidence for the algorithm to perform correctly.

The Fig. 3 shows the spectrum evolution with gradual increase of the Weissenberg number. It can be seen that the flow could become unstable for sufficiently large W even for the values of Re which are below the critical value for Navier–Stokes equations. Two eigenvalues there are marked as A and B and it can be seen that if W is sufficiently large, these two eigenvalues obtain positive real parts, thus indicating the instability of the flow. Note that the spectrum for viscous fluids contain only one unstable mode [31], while here we have at least two. The Fig. 4 shows two unstable modes for these eigenvalues, marked as mode A and mode B respectively. One of that modes (mode A) is symmetrical, and other (mode B) is asymmetrical.

It appears that mode A is the continuation of Tollmien–Schlichting mode [31, 34]. The Fig. 5 shown the trajectory of that mode with change of W. The mode B on the other hand is the continuation of the mode which never become unstable for Navier–Stokes equations, but could become unstable in viscoelastic flow. The same behavior of viscoelastic flow was reported for other rheological models [23, 24], and the fact that this mode become unstable only for that type of fluids allows the one to connect these modes with the instability caused by elastic forces.

Let us now calculate the critical values of parameters for the stability of plane steady flow. Due to the practical purposes we would study the stability of the flow not in the $\mathrm{Re} - \mathrm{W}$ plane but rather in the $\mathrm{Re} - E$ plane, where $E = \mathrm{W}/\mathrm{Re}$ is the elastic number. Unlike W, the value of E is

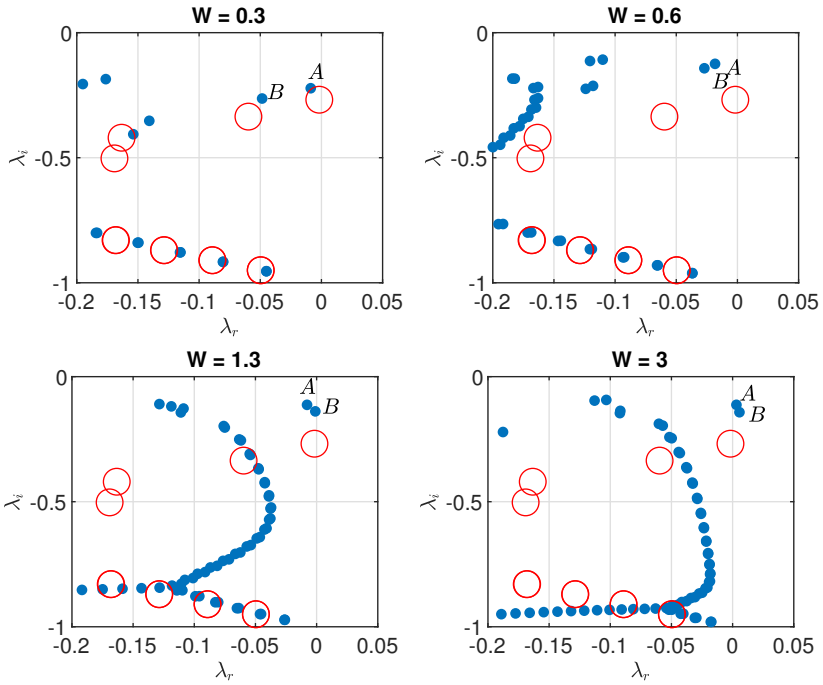

FIG. 3. Spectra of mVP with various W. Red circles are the positions of eigenvalues at W = 0. Re = 5000, $\beta = 0.77$, $\omega = 1$, $\zeta = 0$.

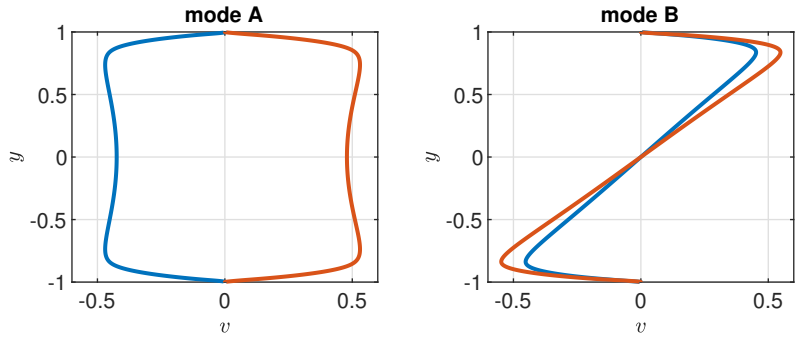

FIG. 4. Unstable modes $v(y)$. Blue – real part, orange – imaginary part. Re = 5000, $\beta = 0.77$, W = 3, $\omega = 1$, $\zeta = 0$.

determined only by rheological properties of the fluid and the geometry of the channel and does not depend on the velocity of the flow, which make it fixed for experimental setup in the slit channel. We will limit the numerical experiments with the maximum value of $\mathrm{Re} = 2 \cdot 10^4$. The higher number of Re decrease the accuracy of the calculations, and in our opinion the chosen

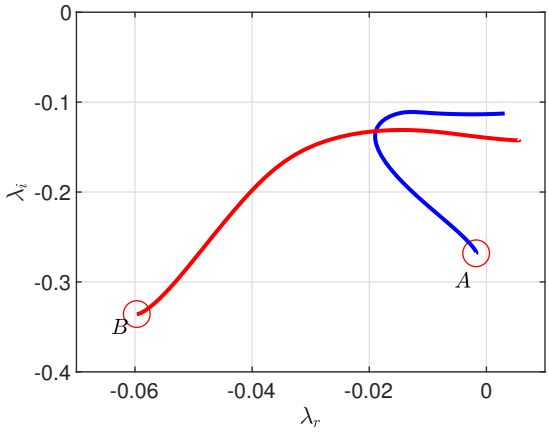

FIG. 5. Trajectories of eigenvalues A and B from $\mathrm{W} = 0$ to $\mathrm{W} = 3$. $\mathrm{Re} = 5000$, $\beta = 0.77$, $\omega = 1$, $\zeta = 0$.

maximum value is enough to describe the general nature of the problem in sufficient details.

The nonlinear terms of constitutive equation of mVP does not allow us to reduce the spectral problem to the two-dimensional one with the help of Squire transformation, which equal this model with other anisotropic rheological models such as Giesecus, FENE-P, PTT [35]. That means, unlike the UCM and Oldroyd-B models, where the Squire theorem is valid, theoretically three-dimensional disturbances in mVP could be more unstable than two-dimensional. Nonetheless, our numerical experiments showed that two-dimensional modes of the problem provide lower critical Reynolds numbers compared to the three-dimensional. So even if we cannot prove that the stability diagram is universally determined by two-dimensional modes, it is true for the cases presented in the paper. The stability zone (Fig. 6) shows that the critical Reynolds number for $E \approx 0$ is indeed close to the one for the newtonean fluid (approximately 5772) but the increase of E causes the rapid grow of critical Re, while even larger E lead to its eventual decrease. Our calculations did not reveal a minimum value of Re which guarantees the stable flow regardless of the E. Apparently, the sufficiently large E can destabilize the flow of any predetermined velocity, which matches with the findings for number of other rheological models [7, 23, 24, 29].

The sharp raise of $\mathrm{Re}-E$ curve at low E happens due to the disappearance of the fragment of neutral stability curve of the eigenmode A (Fig. 7). On this figure it is evident that the neutral stability curve closes and shrinks to nothing with increasing E. The critical value of $E \approx 26 \cdot 10^{-6}$ is when the curve disappears which causes the critical value of Re to jump instantaneously to the next fragment of the stability curve situated somewhere higher than the upper limit of Re at which the calculations were performed. Further increase of E lead to downward movement of neutral stability curves for

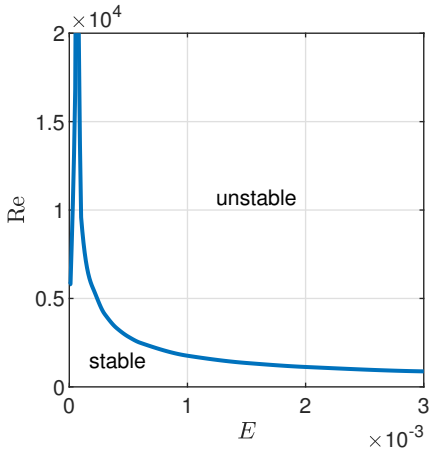

FIG. 6. Zones of stability and instability, $\mathrm{Re} - E$ plane, $\beta = 0.77$.

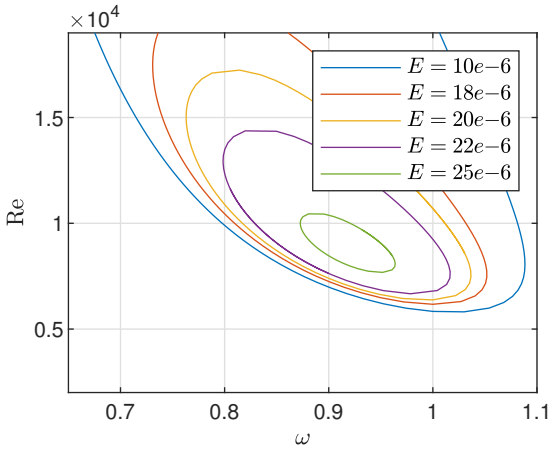

FIG. 7. Neutral stability curves of mode A, $\beta = 0.77$, $\zeta = 0$.

modes A and B, Fig. 8. That figure also presents the neutral stability curves for three-dimensional disturbances $\zeta = 0.1$ and $\zeta = 0.3$. It could be seen that these curves are placed higher than the curves for two-dimensional modes A and B, and thus only two-dimensional modes here determine the critical Reynolds number. Further increase of ζ leads to stability curves quickly leave the area $\mathrm{Re} < 2 \cdot 10^4$. The same result is true for every calculation we performed within this research, even if we cannot be sure that the same outcome is valid for mVP model in general.

3.3. Continuous spectrum. Since our calculations showed that two-dimensional disturbances are key for stability analysis, we will limit the presentation with two-dimensional case in this section.

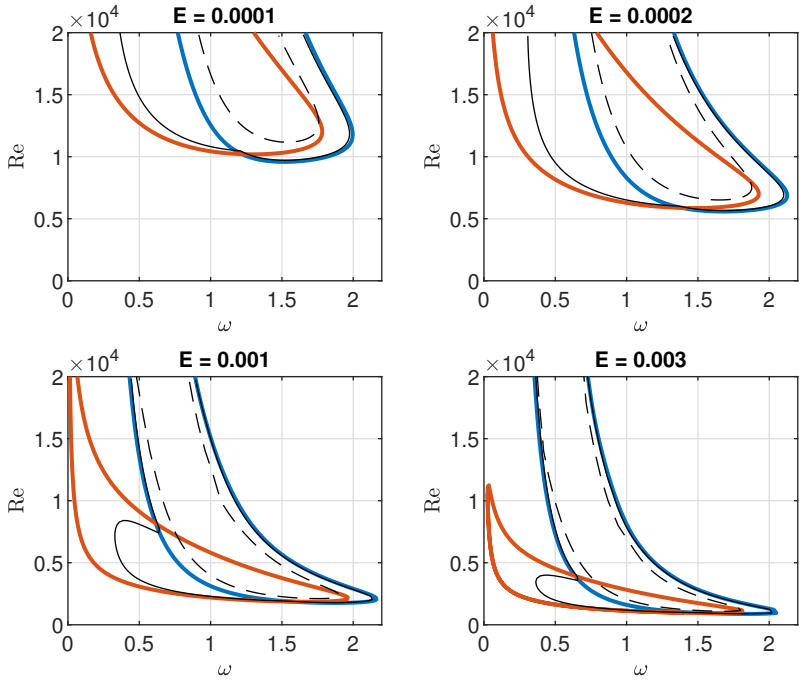

FIG. 8. Neutral stability curves. Blue line for a mode A, orange line for a mode B, $\zeta = 0$. Solid black line is $\zeta = 0.1$, dashed black line is $\zeta = 0.3$. $\beta = 0.77$.

The area of the complex plane shown on the Fig. 9 contains the unstructured cloud of eigenvalues. Numerical experiments with various grid size N reveal that the position of this eigenvalues depend on N and thus the accuracy of calculations for that part of the spectrum is questionable. For better understanding of that part of the spectrum let us rewrite the equations (11)-(13) as

$$\begin{aligned}
&(\omega \mathrm{W}\lambda + A_1)a_{11} + B_1 a_{12} + C_1 a_{22} = V_{10}v + V_{11}v' + V_{12}v'',\\
&A_2 a_{11} + (\omega \mathrm{W}\lambda + B_2)a_{12} + C_2 a_{22} = V_{20}v + V_{22}v'',\\
&A_3 a_{11} + B_3 a_{12} + (\mathrm{W}\lambda + C_3)a_{22} = V_{30}v + V_{31}v'.
\end{aligned} \tag{20}$$

Here, as it follows from (11)-(13), the coefficients A_j, B_j, C_j, V_{j0}, V_{j1}, V_{j2}, $j = 1, 2, 3$ are functions of y according to their dependence on the steady solution U_0. Let

$$M = \begin{pmatrix} \omega \mathrm{W}\lambda + A_1 & B_1 & C_1 \\ A_2 & \omega \mathrm{W}\lambda + B_2 & C_2 \\ A_3 & B_3 & \mathrm{W}\lambda + C_3 \end{pmatrix}.$$

By Cramer's rule,

$$a_{jm} = \frac{\det(M_{jm})}{\det(M)},\ j, m = 1, 2, \tag{21}$$

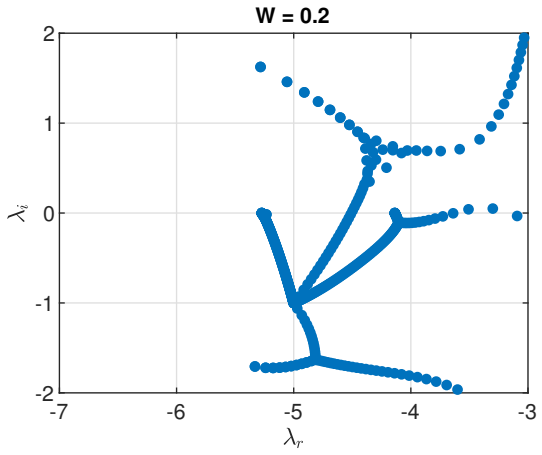

FIG. 9. Fragment of the spectrum at $\mathrm{Re} = 5000, \mathrm{W} = 0.2$, $\beta = 0.77$, $\omega = 1$, $\zeta = 0$.

where M_{jm} is the matrix formed by replacing corresponding column of the matrix M with the vector of right-hand sides of (20). It is clear that $\det M$ is the polynomial of power three of λ with functions of y as coefficients. By substituting (21) to (9), we can see that the resulting equation for v will be linear of the fourth-order since (9) contains a_{12}'' and from (21) it follows that a_{12} in turn linearly depends on v''. The coefficient at $v^{(4)}$ of the resulting equation would be proportional to

$$d_4 = \frac{(\omega \mathrm{W}\lambda + A_1)(\mathrm{W}\lambda + C_3)V_{22}}{\det(M)} - \\ - \frac{A_2(\mathrm{W}\lambda + C_3)A_2V_{12} - V_{12}C_2A_3 + V_{22}A_3C_1}{\det M}. \quad (22)$$

Note that the coefficient at $v^{(3)}$ of that equation would contain the term proportional to d_4'. By multiplying the equation by $(\det M)^2$, we get that the coefficient at $v^{(4)}$ would be zero if either numerator of d_4 is zero or $\det M = 0$, while the coefficient of $v^{(3)}$ would be non-zero in both cases. That makes the roots of 5th-order equation

$$((\omega \mathrm{W}\lambda + A_1)(\mathrm{W}\lambda + C_3)V_{22} - A_2(\mathrm{W}\lambda + C_3)A_2V_{12} + \\ + V_{12}C_2A_3 - V_{22}A_3C_1) \det M = 0 \quad (23)$$

the eigenvalues of (9)-(17). Since the coefficients of (23) are functions of y, we have the continuous spectrum of (9)-(17) with five eigenvalues for any y, $-1 \le y \le 1$. By mapping these roots on the Fig. 10 and comparing them with the spectrum calculated in previous subsection, we can see that the correlation between the two is present. The ends of branches of continuous spectrum are captured with numerical algorithm, while the rest of numerical eigenvalues create the unstable numerical cloud around continuous spectrum.

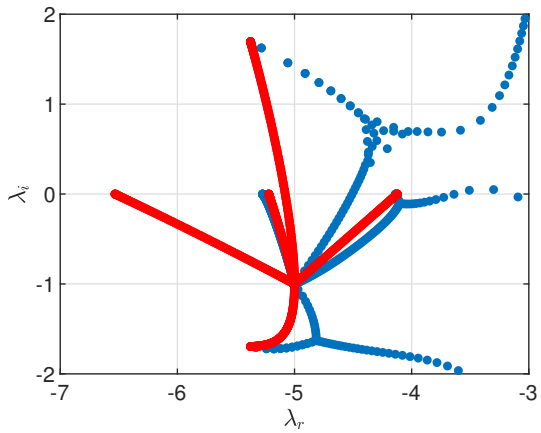

FIG. 10. Numerical spectrum (blue) and solution of (23) (red). $\mathrm{Re} = 5000, \mathrm{W} = 0.2$, $\beta = 0.77$, $\omega = 1$, $\zeta = 0$.

This behavior of spectral methods used on the problems with continuous spectra is known and appear even in the trivial problems. The important thing here is that even numerical algorithm does not capture the continuous spectrum with good accuracy, this spectrum is located in the left complex half-plane and does not provide instability of the steady state.

The continuous spectrum of rheological models has been observed before, see [36, 37, 38] for example. The exact shape of the spectrum strongly depend on the nonlinearity of constitutive equation and thus is unique for the particular model.

Conclusions

The main result of present research we see in calculating the critical values of Reynolds number for Poiseuille-type plane flow modelled by mVP equations. It was discovered that the critical value is finite and greater than zero for all values of Weissenberg number we have checked. The latter indicates that plane Poiseuille-like flow for mVP is not unconditionally unstable. Even more so, the results of our calculations for limit $E \to 0$ provide us with critical value of Re which is identical to the one for Navier–Stokes equations, which both support the accuracy of performed calculations and adequacy of the rheological model itself, since it is expected that the stability of polymer solution with almost absent elastic forces should closely resemble the one for non-elastic viscous fluid. The two unstable modes (symmetric and asymmetric) were discovered, which correlates with the results for UCM and Oldroyd-B. But, unlike the latter, we showed that for mVP the slight increase of Weissenberg number from zero provides stabilizing effect on the plane flow, even if the further increase of W (or E) leads to eventual drop of critical value of Re, apparently to arbitrarily low values. This effect could reflect

the known experimental fact that the addition of small amount of polymer into the viscous solvent delays the appear of turbulence [3], but we assume that further research is required to verify the correlation between these phenomena. Out calculations showed that the two-dimensional disturbances are the most unstable ones, but we cannot say if this fact is true for mVP model in general or there are counter-examples for some particular sets of parameters.

Appendix

The numerical scheme and the approximation of the boundary conditions. The idea of spectral method is to approximate the function on the grid of $N+1$ nodes by interpolating polynomial of power N. The derivatives of the function thus are calculated as derivatives of said polynomial. That is, if the values of function $v(y)$ are known in the nodes of the grid $\vec{y} = \{y_j\}$, $j = 0, \ldots, N$ and $\vec{v}$ is the vector of $v(y_j)$, then the vector

$$\vec{v}^{(n)} = D^n \vec{v}$$

is the approximation of derivative $v^{(n)}$ in the same nodes, where D is the constant differentiation matrix, independent on v. Naturally, the matrix D is singular, since polynomial does not uniquely defined by its derivative. So the uniqueness of the solution of boundary-value problem is established by implementing boundary conditions. In the present research it was done by decomposing the unknown functions into the polynomials which satisfies the boundary conditions of the problem. Namely, by taking conditions (17) into account, we approximate $v(y)$ by polynomial $(1-y^2)q(y)$, where $q(y)$ is the polynomial of power N and

$$q(y_j) = v(y_j)/(1-y_j)^2,\ j = 1, \ldots, N-1,$$
$$q(\pm 1) = 0.$$

It is clear that the (17) would be satisfied with this approximation [32] The derivatives of $v(y)$ in the grid nodes y_j, $j = 1, \ldots, N$ are approximates as

$$v'(y_j) \approx \frac{\mathrm{d}}{\mathrm{d}y}\left((1-y^2)q(y)\right)|_{y=y_j} = -2y_j q(y_j) + (1-y_j^2)q'(y_j),$$

$$v''(y_j) \approx \frac{\partial^2}{\partial y^2}\left((1-y^2)q(y)\right)|_{y=y_j} = -2q(y_j) - 4y_j q'(y_j) + (1-y_j^2)q''(y_j),$$

$$v'''(y_j) \approx \frac{\mathrm{d}^3}{\mathrm{d}y^3}\left((1-y^2)q(y)\right)|_{y=y_j} = -6q'(y_j) - 6y_j q''(y_j) + (1-y_j^2)q'''(y_j),$$

$$v^{(4)}(y_j) \approx \frac{\mathrm{d}^4}{\mathrm{d}y^4}\left((1-y^2)q(y)\right)|_{y=y_j} = -12q''(y_j) - 8y_j q'''(y_j) + (1-y_j^2)q^{(4)}(y_j).$$

The formulas for approximation of the derivatives of fourth order are needed to solve the equations of type (18). Otherwise, the derivatives of the order up to second are sufficient since the problem written in the form (9)-(17) contains only those.

The boundary conditions $q(\pm 1) = 0$ are implemented by removing first and last row and column from differentiation matrices D^n, $n \leq 4$, thus obtaining the regular matrices $\tilde{D^n}$ of the size $N-1 \times N-1$ [32, 33]. As the result, the vectors of derivatives for v in the inner nodes y_j, $j = 1, \ldots, N-1$ are

$$\vec{v}' = \left(-2\mathrm{diag}(\vec{y}\vec{v}) + \mathrm{diag}(1-(\vec{y})^2)\tilde{D}\vec{v}\right)\mathrm{diag}\left(\frac{1}{1-(\vec{y})^2}\right) = S_1\vec{v},$$

$$\vec{v}'' = \left(-2\mathrm{diag}(\vec{v}) - 4\mathrm{diag}(\vec{y})\tilde{D}\vec{v} + \mathrm{diag}(1-(\vec{y})^2)\tilde{D^2}\vec{v}\right)\mathrm{diag}\left(\frac{1}{1-(\vec{y})^2}\right) = S_2\vec{v},$$

etc.

Using that approximation, the problem (9)-(17) would be transformed into (19), where

$$\vec{U} = (v(y_1), \ldots, v(y_{N-1}), w(y_1), \ldots, w(y_{N-1}), a_{11}(y_0), \ldots, a_{11}(y_N), \ldots)^\top,$$

and the length of $\vec{U}$ is $8N+4$. Note that the components $v(y_0) = v(y_N) = 0$ and $w(y_0) = w(y_N) = 0$ are not included in $\vec{U}$ since they are already taken cared of by the interpolation. The matrix M_1 of the size $8N+4 \times 8N+4$ consist of the blocks $M_1 = \{m_{ln}\}$, $l, n = 1, \ldots, 8$,

$$\begin{aligned}
m_{11} &= -i\omega\mathrm{diag}(\vec{u}_0)S_2 + i\omega(\omega^2+\zeta^2)\mathrm{diag}(\vec{u}_0) + i\omega\mathrm{diag}\left(S_2\vec{u}_0\right),\\
m_{12} &= 0,\\
m_{13} &= \left(\omega^2 D\right)_v,\\
m_{14} &= \left(-i\omega D^2 - i\omega(\omega^2+\zeta^2)I\right)_v,\\
m_{15} &= -\left((\omega^2+\zeta^2)I\right)_v, \cdots\\
m_{21} &= -\omega\zeta\mathrm{diag}(\vec{u}_0)S_1 + \omega\zeta\mathrm{diag}(S_1\vec{u}_0),\\
m_{22} &= -i\omega(\omega^2+\zeta^2)\mathrm{diag}(\vec{u}_0),\\
m_{23} &= -i\omega^2\zeta I_v, \cdots\\
m_{31} &= \left(2i\mathrm{W}\mathrm{diag}(\vec{a}_{120})S_2 - 2\omega\left(I/\mathrm{Re} + \mathrm{W}\mathrm{diag}\left(\vec{a}_{110}\right)\right)S_1 - \mathrm{W}\omega\mathrm{diag}\left(D\vec{a}_{110}\right)\right)_h,\\
m_{32} &= -2i\omega\zeta\left(I/\mathrm{Re} + \mathrm{W}\mathrm{diag}\left(\vec{a}_{110}\right)\right) - 2\mathrm{W}\zeta\mathrm{diag}(\vec{a}_{120}),\\
m_{33} &= \omega\left(\mathrm{ReW}\frac{k-\beta}{3}\left(2\mathrm{diag}\left(\vec{a}_{110}\right) + \mathrm{diag}\left(\vec{a}_{220}\right)\right) + I + \right.\\
&+ \left. 2\beta\mathrm{ReW}\mathrm{diag}\left(\vec{a}_{110}\right) + i\mathrm{W}\omega\mathrm{diag}\left(\vec{u}_0\right)\right)_h,
\end{aligned}$$

etc.

Here I is the unity matrix of $N+1 \times N+1$, subscripts "h" and "v" denotes the removal of first and last rows and columns of matrix respectively. Similarly,

the $M_2 = \tilde{m}_{ln}$ is

$$\tilde{m}_{11} = S_2 - (\omega^2 + \zeta^2)\tilde{I},\ \tilde{m}_{21} = -i\zeta S_1,$$
$$\tilde{m}_{22} = (\omega^2 + \zeta^2)\tilde{I},$$
$$\tilde{m}_{33} = \tilde{m}_{44} = \omega \mathrm{W} I_h,$$
$$\tilde{m}_{55} = \tilde{m}_{77} = \tilde{m}_{88} = \mathrm{W} I_h,$$
$$\tilde{m}_{66} = \omega^2 \mathrm{W} I_h,$$

the rest of $\tilde{m}_{ln}$ are zeroes. Here $\tilde{I}$ is the unity matrix of $N-1 \times N-1$. The eigenvalues of (19) are found with "eig" procedure of MATLAB, which utilizes the QZ-method. The method does not rely on inverse matrices and work reliably even if M_1 or M_2 are singular [39].

Validation of the eigenvalues by shooting method. The spectral methods are known for the high accuracy since they use the information in all nodes of the grid to calculate the derivatives of the function. Still, the numerical spectrum could be significantly different from the real one. The method is prone to create phantom eigenvalues which does not present in the actual problem, and the position of the rest of the eigenvalues could also be off. In certain situations up to the half of found spectrum could be discarded as imprecise [34]. One way to filter the ill-calculated eigenvalues is to check the results on the grids of different sizes. In this research we used the grids of the size $N = 100$, $N = 200$ and $N = 400$. Only the eigenvalues independent of the grid size were used for stability analysis. But even the independence of numerical eigenvalues on the N does not guaranteed that these eigenvalues are not numerical artifacts of the algorithm. Another way to check their validity is to calculate them by alternative numerical method of different nature. The shooting method could be used since it does not rely on the calculation of the eigenvalues of large matrices.

Do do so we reduce the system (9)-(13) to one linear fourth-order equation for v with coefficients as functions of y and λ and supplement it with boundary conditions for v. Then we look for the non-zero solution of the boundary-value problem as linear combination of two numerical linearly independent solutions of the equation with two left boundary conditions. The problem has non-trivial solution if these two partial solutions provide a linearly-dependent right boundary conditions.

We used the procedure "ode15s" of MATLAB (variable-step, variable-order solver, see [40]) with method of intermediate orthogonalization of solutions [41] to find two independent solutions. Finally, we used the Newton–Raphson method to calculate the value of λ which provide the non-trivial eigenfunction with the initial guess taken from spectral calculations.

References

[1] M. Doi, S.F. Edwards, The Theory of Polymer Dynamics, Clarendon: Oxford, 1986.

[2] R.B. Bird, C.F. Curtiss, R.C. Armstrong, O. Hassager, *Dynamics of Polymeric Liquids, Vol. 2*, Wiley, New York, 1987.
[3] D. Samanta, Y. Dubief, M. Holzner, C. Schдfer, A.N. Morozov, C.Wagner, B. Hof, *Elasto-inertial turbulence*, Proceedings of the National Academy of Sciences, **110**:26 (2013), 10557–10562.
[4] S.S. Srinivas, V. Kumaran, 2017 *Effect of viscoelasticity on the soft-wall transition and turbulence in a microchannel*. J. Fluid Mech., **812** (2017), 1076–1118.
[5] J.G. Oldroyd, *On the formulation of rheological equations of state*, Proc. R. Soc., **200**:1063, 523–541.
[6] E.S.G. Shaqfeh, *Purely elastic instabilities in viscometric flows*, Annual Review of Fluid Mechanics, **28**:1 (1996), 129–185.
[7] H.A. Castillo Sanchez, M.R. Jovanovic, S. Kumar, A. Morozov, V. Shankar, G. Subramanian, H.J. Wilson, *Understanding viscoelastic flow instabilities: Oldroyd-B and beyond*, J. Non-Newtonian Fluid Mech., **302** (2022), 104742.
[8] R. Sureshkumar, A.N. Beris, *Linear stability analysis of viscoelastic Poiseuille flow using an Arnoldi-based orthogonalization algorithm*, J. Non-Newtonian Fluid Mech., **56** (1995), 151–182.
[9] R.G. Larson, *Instabilities in viscoelastic flows*, Rheola Acta, **31** (1992), 213–263.
[10] A. Ramachandran, D. T. Leighton, *The influence of secondary flows induced by normal stress differences on the shear-induced migration of particles in concentrated suspensions*, J. Fluid Mech., **603** (2008), 207243.
[11] V.N. Pokrovskii, *The mesoscopic theory of polymer dynamics*, Springer, London, 2010.
[12] Yu.A. Altukhov, A.S. Gusev, G.V. Pyshnograi, *Vvedeniye v mezoskopicheskuyu teoriyu tekuchikh polimernykh sistem*, Barnaul: AltGPA, 2012 (in Russian).
[13] M.A. Makarova, A.S. Malygina, G.V. Pyshnograi, G.O. Rudakov, *Simulation of rheological properties of polyethylene melts under uniaxial tension*, J. Appl. Mech. Tech. Phys., **62** (2021), 1063–1071.
[14] G.V. Pyshnograi, N. A. Cherpakova, H.N.A.A. Joda, *Special features of nonlinear behavior of a polymer solution on large periodic deformations*, J. Eng. Phys. Thermophys., **93** (2020), 617–625.
[15] K. Koshelev, A. Kuznetcov, D. Merzlikina, G. Pyshnograi, I. Pyshnograi, M. Y. Tolstykh, *Mesoscopic rhelogical model for polymeric media flows*, J. Phys.: Conf. Ser., **790** (2017), 012014.
[16] D. A. Merzlikina, G. V. Pyshnograi, R. Pivokonskii, P. Filip, *Rheological model for describing viscometric flows of melts of branched polymers*, J. Eng. Phys. Thermophys., **89** (2016), 652–659.
[17] A.M. Blokhin, A.V. Yegitov, D.L. Tkachev, *Linear instability of solutions in a mathematical model describing polymer flows in an infinite channel*, Comput. Math. and Math. Phys., **55**:5 (2015), 848–873.
[18] D.L. Tkachev, E.A. Biberdorf, *Spectrum of a problem about the flow of a polymeric viscoelastic fluid in a cylindrical channel (Vinogradov-Pokrovski model)*, Siberian Electronic Mathematical Reports, **20**:2 (2023), 1269–1289.
[19] D.L. Tkachev, *Spectrum and linear Lyapunov instability of a resting state for flows of an incompressible polymeric fluid*, J. of Mathematical Analysis and Applications, **522**:1 (2023), 126914.
[20] R.E. Semenko, *Stabilization of the at Poiseuille-type flow for viscoelastic polymeric liquid*, Phys. Fluids, **35** (2023), 033112.
[21] I.E. Golovicheva, S.A. Zinovich, G.V. Pyshnograi, *Effect of the molecular mass on the shear and longitudinal viscosity of linear polymers*, J. Appl. Mech. Tech. Phys., **41** (2000), 347–352.
[22] A.M. Blokhin, N.V. Bambaeva, *Stationary solutions equations of an incompressible viscoelastic polymer liquid*, Comput. Math. and Mach. Phys, **54**:5 (2014), 874–899.

[23] K.C. Porteous, M.M. Denn, *Linear stability of plane Poiseuille flow of viscoelastic liquids*, Transactions of the Society of Rheology, **16**:2 (1972), 295–308.
[24] I. Chaudhary, P. Garg, V. Shankar, G. Subramanian, *Elasto-inertial wall mode instabilities in viscoelastic plane Poiseuille flow*, J. Fluid Mech, **881** (2019), 119–163.
[25] Yu.A. Altukhov, G.V. Pyshnograi, I.G. Pyshnograi, *Slipping phenomenon in polymeric fluids ow between parallel planes* , World Journ. of Mech., **1** (2011), 294–298.
[26] T. Sochi, *Slip at fluid-solid interface*, Polymer Rev., **51**:4 (2011), 309–340.
[27] V. A. Gorodtsov, A. I. Leonov, *On a linear instability of a plane parallel Couette flow of viscoelastic fluid*, J. Applied Mathematics and Mechanics, **31**:2 (1967), 289–299.
[28] R.J. Hansen, R. Little, P.G. Forame, *Experimental and theoretical studies of early turbulence*, Journal of Chemical Engineering of Japan, **6**:4 (1973), 310–314.
[29] G. Buza, J. Page, R.R. Kerswell, *Weakly nonlinear analysis of the viscoelastic instability in channel flow for finite and vanishing Reynolds numbers*, J. Fluid Mech., **940** (2022), A11.
[30] J. Azaiez, G. M. Homsy, *Linear stability of free shear flow of viscoelastic liquids*, J. Fluid Mech., **268** (1994), 37–69.
[31] P. G. Drazin, *Introduction to Hydrodynamic Stability*, Cambridge University Press, Cambridge, 2002.
[32] J.P. Boyd, *Chebyshev and Fourier Spectral Methods.*, Springer Berlin, Heidelberg, 1989.
[33] L.N. Trefethen, *Spectral methods in MATLAB*, SIAM, Philadelphia, 2000.
[34] P.J. Schmid, D.S. Henningson, *Stability and Transition in Shear Flows*, Springer Science+Business Media, New York, 2001.
[35] L. J. da Silva Furlan, M. de Mendonca, M.de Araujo, L. de Souza, *On the validity of Squire's theorem for viscoelastic fluid flows*, J. Non-Newtonian Fluid Mech., **307** (2022), 104880.
[36] M. Renardy, Y. Renardy, *Linear stability of plane Couette flow of an upper convected Maxwell fluid*, J. Non-Newtonian Fluid Mech., **22** (1986), 23–33.
[37] H.J. Wilson, M. Renardy, Y. Renardy, *Structure of the spectrum in zero Reynolds number shear flow of the UCM and Oldroyd-B liquids*, J. Non-Newtonian Fluid Mech., **80** (1999), 251–268.
[38] M.D. Graham, *Effect of axial flow on viscoelastic Taylor–Couette instability*, J. Fluid Mech., **360** (1998), 341–374.
[39] D. Kressner, *Numerical Methods for General and Structured Eigenvalue Problems*, Springer-Verlag Berlin, Heidelberg, 2005.
[40] L.F. Shampine, M.W. Reichelt, J.A. Kierzenka, *Solving Index-1 DAEs in MATLAB and Simulink*, SIAM Review, **41** (1999), 538–552.
[41] S.K. Godunov, *O chislennom reshenii krayevykh zadach dlya sistem obyknovennykh differentsialnykh uravneniy*, Usp. Mat. Nauk., **16** (1961), 171–174 (in Russian).

Roman Evgenievich Semenko
Sobolev Institute of Mathematics,
pr. Koptyuga, 4,
630090, Novosibirsk, Russia
Email address: r.e.semenko@math.nsc.ru

Giyosiddin N. Shukurov
Novosibrsk State University,
Pirogova st., 1,
630090, Novosibirsk, Russia
Email address: g.shukurov@g.nsu.ru